future transportation

MDPI

Article

Network-Level Traffic and Safety Effects of Automated Vehicle Market Penetration Under Take-Over Events: A Microsimulation Study

Marios Sekadakis *, Dimitrios Nikolaou and George Yannis

Department of Transportation Planning and Engineering, National Technical University of Athens, 5 Heroon Polytechniou Str., GR-15773 Athens, Greece; dnikolaou@mail.ntua.gr (D.N.); geyannis@central.ntua.gr (G.Y.)
* Correspondence: msekadakis@mail.ntua.gr

Abstract

This study investigates the network-level traffic and safety effects of increasing Market Penetration Rate (MPR) of SAE Level 2 and Level 3 automated vehicles under take-over conditions. A calibrated microsimulation model of a real-world 50 km highway corridor in Greece (Nea Odos) was used to develop 18 scenarios combining two take-over contexts (Lane Closure and ODD Exit), two Time Budget (TB) configurations, and four MPR levels (25–100%), complemented by two baselines. Traffic performance was assessed through five network-level indicators (speed, delay, lane-changing frequency, travel time, and density). Safety was evaluated through 674 conflict events extracted via the Surrogate Safety Assessment Model (SSAM), using Time-to-Collision (TTC) as the primary indicator. MPR is the dominant feature of both dimensions. Increasing MPR produces a monotonic reduction in speed (−19.2% at 100% MPR), a sharp decline in lane-changing (−59.8%), and increases in density (+21.1%) and travel time (+22.4%), delay peaks non-monotonically at 50% MPR (+107.9%). Spearman correlations between MPR and the traffic indicators are very strong for speed, lane changes, travel time, and density, while delay time yields a weaker correlation reflecting its non-monotonic response. All operating points remain within free-flow conditions throughout the MPR range. The MPR effect on TTC is marginal (p = 0.065) but non-monotonic, with 75% MPR yielding significantly higher mean TTC than 50% and 100% MPR. Neither TB duration nor TOR context produces a statistically significant effect on traffic indicators or TTC distributions, with negligible effect sizes in both cases. Traffic costs of mixed-traffic automation appear at partial penetration, while network-level safety benefits remain limited and non-linear.

Keywords: automated vehicles; market penetration rate; take-over request; mixed traffic; microsimulation; traffic performance; surrogate safety measures; time-to-collision

Check for updates

Academic Editor: Jian Ma

Received: 23 July 2026
Revised: 13 August 2026
Accepted: 18 August 2026
Published: 24 August 2026

Copyright: © 2026 by the authors. Licensee MDPI, Basel, Switzerland. This article is an open access article distributed under the terms and conditions of the Creative Commons Attribution (CC BY) license.

1. Introduction

The accelerating deployment of partially automated vehicles, particularly those operating at SAE Levels 2 and 3, is reshaping the composition of traffic on motorways and urban arterials. As these systems move from controlled pilots into real-world mixed-traffic conditions, road networks are increasingly populated by fleets in which automated and human-driven vehicles interact continuously, and in which automated vehicles must intermittently return control to the driver in response to system limits or environmental triggers. Understanding how such transitions propagate from the individual driver to the

surrounding traffic stream has therefore become a central concern for traffic engineers and policymakers. While a substantial body of human-factors research has examined Take-Over Requests (TORs) at the driver level, comparatively little is known about their aggregate consequences for network performance. This disconnect between micro-level behavioural evidence and macro-level operational outcomes motivates the present study, which seeks to bridge driver-level TOR dynamics and network-level traffic effects within a unified microsimulation framework.

A substantial microsimulation literature has examined how the Market Penetration Rate (MPR) of Connected and Automated Vehicles (CAVs) reshapes traffic stability, speed, flow, and surrogate safety indicators such as Time-to-Collision (TTC) and Post-Encroachment Time (PET). The prevailing finding is that higher CAV shares smooth traffic flow, reduce stop-and-go waves, raise average speeds and throughput, and reduce conflict rates and surrogate crash risk [1–10]. These effects are, however, markedly non-linear: at low to moderate MPRs (below roughly 30% to 40%), improvements are small or even adverse because of complex interactions between Human-Driven Vehicles (HDVs) and CAVs, and the positive effects become consistent only once a critical mass is reached [7–9,11–13]. These findings directly motivate the four MPR levels adopted in this study, which span the critical 25–100% range where both traffic and safety effects are expected to be most pronounced and non-linear.

The same pattern recurs across individual performance dimensions. Increasing MPR enhances string stability by reducing oscillations and smoothing trajectories [2,3,14–16], with notable gains once CAVs exceed roughly 40% to 50% of the fleet [3,17], below this threshold, heterogeneous behaviour can introduce instability [7,17]. Average speeds and throughput follow a similar trajectory, rising clearly above the 40% to 50% range but remaining negligible or slightly adverse below it [4,6,13,18–20], with dedicated lanes and platooning offering additional gains under specific conditions [21]. Surrogate safety measures show the strongest dose-response: meta-analytic evidence reports roughly 4% fewer conflicts at 10% MPR, around 17% at 50%, and over 40% at 90% MPR [9,22], although a few studies report transient increases in conflicts at very low MPRs before benefits emerge [7,23]. These dose-response patterns provide the reference framework against which the surrogate safety outcomes of this study are interpreted.

These network-level outcomes are sensitive to a broad set of moderators, including communication reliability, heavy-vehicle share, platoon size, lane-management strategy, network topology, and aggressive lane-changing policies [6,21,24–27]. Crucially, behavioural adaptation of human drivers to growing automation shares, which has been shown experimentally to alter following distances and reaction times in mixed fleets [28], is often omitted from simulation models, and full-scale safety gains typically require near-complete automation above 80% to 90% MPR [8,9,22]. A further limitation, central to the present study, is that MPR is almost universally treated as a static parameter, with the dynamic transitions between automated and manual control associated with TORs left outside the simulation framework. This gap motivates the core methodological contribution of the present study, which embeds dynamic TOR events within a calibrated mixed-traffic simulation rather than treating MPR as a fixed parameter.

Take-Over Requests (TORs) in conditionally automated vehicles have been studied extensively at the driver level, and three factors emerge as the principal determinants of post-TOR behaviour and safety: the take-over Time Budget (TB), the variability of driver response, and the nature of the triggering event, such as an Operational Design Domain (ODD) exit versus a lane closure or sudden system failure [29–35].

Longer TBs generally allow drivers to regain situation awareness and execute smoother control transitions, with several studies recommending dynamic or scenario-adaptive lead

times of roughly 7 to 30 s for non-critical events such as planned ODD exits [30–37]. Shorter TBs of less than about seven seconds yield faster reactions but poorer take-over quality and a higher incidence of unsafe manoeuvres [29,32,38], and excessively long budgets may reduce alertness or invite procrastination [30,36]. Driver response is highly heterogeneous. Take-Over Time (TOT) and quality vary with engagement in Non-Driving-Related Tasks (NDRTs), particularly visual or cognitive ones, with traffic complexity, TOR modality, prior exposure, age, trust in automation, cognitive load, and individual crash-risk profile [38–43]. High-load or multiple NDRTs significantly delay responses and degrade control, whereas multimodal TORs can moderate these effects [40,44]. However, the present study focuses on the network-level consequences of TB duration rather than its driver-level determinants, using empirically derived post-TOR behavioural profiles to parameterise heterogeneous human response [45,46].

Direct comparisons of triggering events show that drivers respond more quickly to urgent lane closures or system failures than to scheduled ODD exits, but lateral control is smoother under planned transitions, with no significant difference reported for longitudinal performance [29]. Post-TOR driving remains impaired for several minutes after the transition, especially following NDRT engagement, with elevated lane deviations and degraded control [47], repeated exposure improves reaction times without fully restoring pre-transition driving quality [48]. Taken together, these findings motivate adaptive TOR designs that account for scenario urgency, driver state, and environmental complexity [49], and underscore that the TB and the TOR context are the two design levers most likely to shape network-level outcomes once driver-level transitions are embedded in a microsimulation framework. These two factors, TB duration and TOR context, therefore constitute the primary experimental variables of the present study, alongside MPR, enabling a systematic assessment of their joint network-level consequences.

Prior work by the present authors provides the empirical foundation for translating these driver-level findings into microsimulation inputs. Sekadakis et al. used a driving-simulator experiment to identify distinct post-TOR response categories among SAE Level 2 and 3 drivers, supplying the behavioural profiles required to parameterise heterogeneous human response after a take-over [45]. Moreover, through a systematic review and meta-analysis of take-over time at SAE Levels 2 and 3, the empirical distribution of TB values used to define the influence of short and extended take-over windows was established [46]. Together these two studies allow TOR dynamics to be embedded in a calibrated network simulation in a way that is grounded in observed driver behaviour rather than assumed.

Taken together, the literature reviewed above reveals a clear gap. Existing mixed-traffic microsimulation studies typically treat MPR as a static parameter and omit the dynamic behavioural transitions associated with TORs, while the TOR literature itself remains largely confined to driver-level outcomes observed in isolation from network conditions. As a result, no study to date has simultaneously quantified the traffic and safety effects of MPR under dynamic TOR conditions on a real, calibrated corridor. The present work is also distinct from the companion safety analysis by Sekadakis et al. [50], which examined conflict-level outcomes through a spatial Generalised Additive Model (sGAM), here, the focus shifts from localised conflict mechanisms to a joint network-level assessment of traffic performance and aggregated safety indicators across MPR and TB conditions.

Against this background, the present study pursues three objectives. First, it assesses how MPR, including the non-linear behaviour reported in the literature at low and intermediate penetration levels, shapes five traffic performance indicators, namely speed, travel time, density, delay time, and lane-changing activity, under representative TOR conditions on a calibrated corridor. Second, it characterises TTC based safety conflict patterns across combinations of MPR, TB, and TOR context, providing a network-level

view of how automation share and transition timing jointly influence conflict exposure. Third, it tests whether TB and TOR context produce statistically distinguishable effects on either the traffic or the safety dimension, thereby clarifying which design and policy levers most strongly mediate the network impact of TORs. The remainder of the paper is organised as follows: Section 2 describes the simulation network, calibration, TOR emulation, scenarios, and analytical methods, Section 3 presents the traffic and safety results, Section 4 discusses traffic and safety implications together with the study's limitations, and Section 5 concludes.

2. Methodology

2.1. Simulation Network and Calibration

The simulation environment is a calibrated Aimsun Next microsimulation model of a 50 km section of the Nea Odos motorway forming part of the Athens-Thessaloniki corridor in central Greece (Figure 1). The modelled section comprises six entry and exit points (Thiva, Akrefnio, Kastro, Martino, Malesina, Traganas), two lanes per direction separated by a central median, and a posted speed limit of 120 km/h. Network geometry was extracted from OpenStreetMap and cross-validated using Google Maps (Figure 2). The model was calibrated with hourly traffic data from eleven representative mid-weekdays (October 2021) provided by the operator Nea Odos S.A. The simulation period corresponds to the peak hour (14:00–15:00), during which demand reached approximately 1700 vehicles per hour per direction. Flow calibration achieved 91.7% of links with GEH < 5 and 100% with GEH < 10, the regression of simulated versus observed volumes yielded $R^2 = 0.96$. Speed validation produced an average deviation of 4%. The calibrated demand comprised 1782 trips: 74% light vehicles, 22% heavy goods vehicles, 3% motorcycles, and 1% buses. Full details are reported in Sekadakis et al. [50].



Figure 1. Real section of the Nea Odos highway between Athens and Thessaloniki (Source: OpenStreetMap and Google Maps) [50].

2.2. TOR Emulation and Vehicle Parameterisation

A custom Python 3.10 API was developed to implement TOR events within Aimsun Next by dynamically modifying vehicle behavioural parameters (deceleration, clearance, gap acceptance, reaction time) at predefined trigger sections. Two TOR contexts were modelled: a Lane Closure scenario triggering a lane-change manoeuvre through a temporary road-works section, and an ODD Exit scenario where automation disengaged at an operational design domain boundary without a mandatory lane change. Both trigger sections were spatially coincident. Following the TB period, vehicles entered a manual-driving phase for a fixed 3 km before automated parameters were restored.

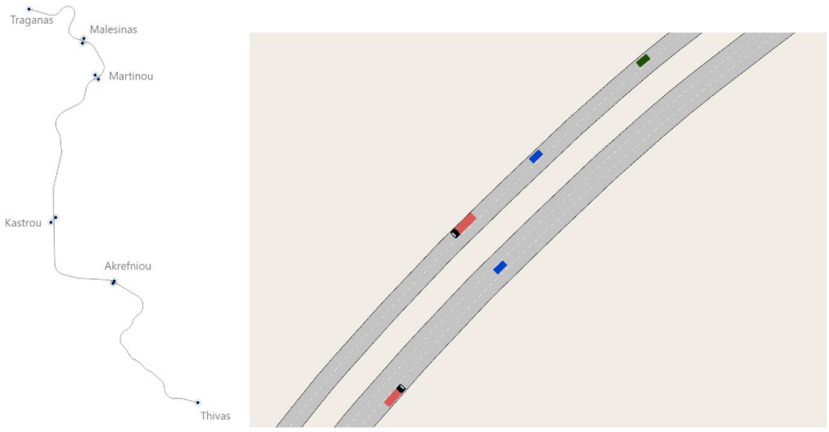


Figure 2. Simulated Aimsun Next network including ramps, merge zones, and traffic detectors [50].

Post-TOR behavioural profiles were derived from a high-fidelity driving simulator experiment reported in Sekadakis et al., 2025 [45], in which participants drove under SAE Level 2 and Level 3 automation before responding to unexpected TOR events under varying HMI conditions. High-frequency kinematic data, including speed, acceleration, deceleration, and lane position, were recorded at each time step throughout the take-over sequence. A sequential analytical pipeline was applied to these data: Principal Component Analysis (PCA) was first used to reduce the dimensionality of the kinematic feature space, k-means clustering was then applied to the principal component scores to identify natural groupings in driver response patterns, and Linear Discriminant Analysis (LDA) was used to validate and characterise the resulting clusters. This pipeline yielded three statistically distinct and internally consistent post-TOR behavioural profiles:

i. The Passive and Slow Response profile is characterised by low deceleration magnitudes (maximum deceleration 1.06 m/s^2 for Level 2 and 0.65 m/s^2 for Level 3), reflecting delayed and cautious re-engagement. Drivers in this group exhibited prolonged reaction times and conservative braking behaviour, suggesting incomplete situational awareness recovery at the point of manual control assumption.
ii. The Nervous and Moderate Response profile is characterised by high and abrupt deceleration (maximum deceleration 5.15 m/s^2 for Level 2 and 5.43 m/s^2 for Level 3), reflecting an urgent and destabilising response to the TOR. This profile generates the greatest speed differentials with surrounding traffic and is associated with the highest short-term conflict risk.
iii. The Normal and Quick Response profile is characterised by moderate and controlled deceleration (maximum deceleration 0.94 m/s^2 for Level 2 and 0.80 m/s^2 for Level 3), reflecting smooth and timely re-engagement with minimal disruption to traffic flow.

Under Level 2 automation, the empirical distribution of profiles was 57% Normal, 33% Passive, and 10% Nervous, reflecting the shorter TB (5s) and higher driver engagement typically associated with Level 2 systems. Under Level 3 automation, the distribution shifted to 44% Normal, 46% Passive, and 10% Nervous, consistent with the longer TB (15s) and greater automation reliance that characterises Level 3, which tends to reduce driver readiness at the moment of the TOR. These proportions were held constant across all scenarios to preserve behavioural consistency between TOR contexts and MPR levels. In the simulation, profile assignment was applied probabilistically at the vehicle level, and Gaussian sampling around profile-specific means for deceleration and clearance was used to introduce inter-driver variability within each profile class, ensuring that vehicles sharing the same profile still exhibited heterogeneous trajectories. Full parameter values for each profile and automation level are reported in Tables 1 and 2 of the companion study [50].

Table 1. Simulation scenario matrix.

Sc.	Context	MPR	TB (L2)	TB (L3)	L2 Share	L3 Share
1	**Baseline LC**	**0%**	**–**	**–**	**–**	**–**
2	Lane Closure	25%	5 s	15 s	80%	20%
3	Lane Closure	50%	5 s	15 s	60%	40%
4	Lane Closure	75%	5 s	15 s	40%	60%
5	Lane Closure	100%	5 s	15 s	20%	80%
6	Lane Closure	25%	7 s	20 s	80%	20%
7	Lane Closure	50%	7 s	20 s	60%	40%
8	Lane Closure	75%	7 s	20 s	40%	60%
9	Lane Closure	100%	7 s	20 s	20%	80%
10	**Baseline ODD**	**0%**	**–**	**–**	**–**	**–**
11	ODD Exit	25%	5 s	15 s	80%	20%
12	ODD Exit	50%	5 s	15 s	60%	40%
13	ODD Exit	75%	5 s	15 s	40%	60%
14	ODD Exit	100%	5 s	15 s	20%	80%
15	ODD Exit	25%	7 s	20 s	80%	20%
16	ODD Exit	50%	7 s	20 s	60%	40%
17	ODD Exit	75%	7 s	20 s	40%	60%
18	ODD Exit	100%	7 s	20 s	20%	80%

MPR = Market Penetration Rate. TB (L2)/TB (L3) = Time Budget for Level 2 and Level 3 vehicles. L2/L3 share = proportion of each automation level within the automated-vehicle fleet. Baseline scenarios contain no automated vehicles. Bold rows indicate baseline scenarios with no automation.

Table 2. Network-level traffic performance indicators by scenario.

Sc.	Context	MPR	TB	Speed (km/h)		Delay (s/km)		Lane ch. (No/km)		Travel t. (s/km)		Density (veh/km)	
				Value	Δ%	Value	Δ%	Value	Δ%	Value	Δ%	Value	Δ%
1	Baseline LC	0%	–	100.39	+0.0	0.63	+0.0	104.46	+0.0	36.43	+0.0	2.32	+0.0
2	LC	25%	Reg	94.48	−5.9	1.16	+84.1	106.36	+1.8	38.82	+6.6	2.48	+6.9
3	LC	50%	Reg	89.47	−10.9	1.31	+107.9	90.34	−13.5	40.93	+12.4	2.62	+12.9
4	LC	75%	Reg	85.12	−15.2	1.07	+69.8	66.15	−36.7	42.81	+17.5	2.72	+17.2
5	LC	100%	Reg	81.08	−19.2	0.68	+7.9	41.98	−59.8	44.60	+22.4	2.81	+21.1
6	LC	25%	Ext	94.62	−5.7	1.12	+77.8	107.72	+3.1	38.77	+6.4	2.48	+6.9
7	LC	50%	Ext	89.75	−10.6	1.21	+92.1	92.40	−11.5	40.82	+12.1	2.61	+12.5
8	LC	75%	Ext	85.42	−14.9	0.96	+52.4	67.78	−35.1	42.69	+17.2	2.72	+17.2
9	LC	100%	Ext	81.23	−19.1	0.61	−3.2	42.21	−59.6	44.53	+22.2	2.81	+21.1
10	Baseline ODD	0%	–	100.45	+0.1	0.61	−3.2	104.00	−0.4	36.41	−0.1	2.32	+0.0
11	ODD	25%	Reg	94.52	−5.8	1.14	+81.0	105.79	+1.3	38.81	+6.5	2.48	+6.9
12	ODD	50%	Reg	89.50	−10.8	1.29	+104.8	89.48	−14.3	40.91	+12.3	2.62	+12.9
13	ODD	75%	Reg	85.18	−15.2	1.04	+65.1	65.96	−36.9	42.78	+17.4	2.72	+17.2
14	ODD	100%	Reg	81.13	−19.2	0.65	+3.2	41.72	−60.1	44.57	+22.3	2.81	+21.1
15	ODD	25%	Ext	94.52	−5.8	1.15	+82.5	105.88	+1.4	38.81	+6.5	2.48	+6.9
16	ODD	50%	Ext	89.51	−10.8	1.29	+104.8	89.47	−14.3	40.91	+12.3	2.62	+12.9
17	ODD	75%	Ext	85.17	−15.2	1.05	+66.7	65.87	−36.9	42.79	+17.5	2.72	+17.2
18	ODD	100%	Ext	81.13	−19.2	0.65	+3.2	41.74	−60.0	44.57	+22.3	2.81	+21.1

MPR = Market Penetration Rate. TB = Time Budget (Reg = Regular, Ext = Extended). Δ% = percentage change relative to Scenario 1 (Baseline LC).

The behavioural parameters adopted in this study represent the best currently available empirical grounding, with each parameter class traced to an explicit empirical or literature-based source. Automation-level control parameters were sourced from Xie et al. [51] and Zhang [52]: for Level 2 maximum deceleration was set to 2.5 m/s^2 and reaction time to 1.0 s and for Level 3 maximum deceleration was 2.75 m/s^2 and reaction time to 0.5 s, consistent with the higher longitudinal control capability of higher-level automation. Post-TOR behavioural profiles were derived from our driving simulator experiment [48], which applied a sequential PCA-k-means-LDA pipeline to high-frequency kinematic data to identify three statistically distinct response classes Passive, Nervous, and Normal characterised by distinct deceleration magnitudes (maximum deceleration ranging from 0.65 to 5.43 m/s^2 across profiles for Level 3), clearance values, and reaction times, as

reported in full in Tables 1 and 2 of the companion study [50]. Gaussian sampling around profile-specific means was applied to each parameter to replicate inter-driver heterogeneity, ensuring that vehicles sharing the same post-TOR profile still exhibited heterogeneous trajectories. Manual driving parameters correspond to calibrated Aimsun defaults, consistent with standard practice in microsimulation. No core safety-sensitive parameter was assigned without empirical or literature-based justification. While simulator-derived post-TOR parameters carry inherent ecological validity limitations relative to naturalistic deployment data, which does not yet exist at the granularity required for L2/L3 microsimulation parameterisation, they constitute the only source of controlled, scenario-specific post-TOR kinematic data currently available in the published literature, and this limitation is further discussed in Section 4.3.

2.3. Simulation Scenarios

A total of 18 scenarios were developed by combining two TOR contexts, two TB configurations (Regular and Extended), and four MPR levels (25–100%), plus two baseline scenarios with 100% human-driven traffic (Table 1). Regular TB corresponded to 5 s (Level 2) and 15 s (Level 3), Extended TB to 7 s and 20 s, derived from the meta-analytic relationship in Sekadakis & Yannis [46]. Each scenario was run with 10 replications, the representative replication closest to the cross-replication mean travel time was selected for indicator extraction.

The 18 scenarios arise from the full factorial combination of two TOR contexts, two TB configurations, and four MPR levels, complemented by two baseline conditions, ensuring balanced and systematic coverage of the primary experimental dimensions of interest. The two TOR contexts, Lane Closure and ODD Exit, were selected on the basis of the systematic review and meta-analysis by Sekadakis and Yannis [46], which identified these as the two most frequently investigated TOR triggering conditions in the empirical literature. The Regular TB values of 5 s for Level 2 and 15 s for Level 3 correspond to the empirical TOT distributions measured in Sekadakis et al. [45], while the Extended TB values of 7 s and 20 s were derived from the meta-analytic relationship proposed in Sekadakis and Yannis [46], corresponding to an approximate 1.8% increase in the mean and standard deviation of the TOT distribution. The three post-TOR behavioural profiles and their mixture proportions were likewise derived directly from the empirical distributions reported in Sekadakis et al. [45], with each experimental factor therefore traceable to a specific measured or analytically derived empirical source.

2.4. Traffic Performance Indicators

Five network-level traffic indicators were extracted from Aimsun Next outputs and aggregated across all vehicle types and the full corridor: (i) Speed (km/h), arithmetic mean network speed, (ii) Delay Time (s/km), mean excess travel time per kilometre, (iii) Lane Changes (#/km), normalised lane-change frequency, (iv) Travel Time (s/km), mean time to traverse one kilometre, and (v) Density (veh/km), mean vehicle density. These were selected from 28 available Aimsun outputs based on variability across scenarios (CV > 2%), absence of redundancy, and traffic policy relevance. Indicators that were constant (Number of Stops, Waiting Time), near-constant (Input Count/Flow, CV < 0.5%), or expressed as linear transformations of retained indicators (Total Travel Time, Total Lane Changes) were excluded. As Aimsun standard deviations reflect within-simulation temporal variability rather than cross-replication uncertainty, formal statistical testing of traffic differences is not feasible, Spearman rank correlations between MPR and each indicator are reported instead.

2.5. Safety Conflict Extraction and Analysis

Conflict events were extracted from Aimsun Next v24 trajectory files using SSAM v3.0 with standard thresholds (TTC $\leq$ 1.5 s, PET $\leq$ 5.0 s), as originally proposed by Gettman & Head (2003) [53]. TTC values $\leq$ 0.1 s were excluded as simulation artefacts. The minimum TTC per interaction was retained as the conflict severity measure. TTC is discretised at 0.1 s intervals in SSAM output, 23.1% of conflicts occur at the lower bound of 0.2 s, indicating left-censoring. The natural logarithm of TTC was used for statistical analysis. Three non-parametric tests were applied: (i) Kruskal-Wallis to assess the overall MPR effect on log(TTC) across four MPR levels, (ii) directional Mann-Whitney U tests to examine the 75% MPR safety advantage over 50% and 100% MPR (one-sided), and (iii) two-sided Mann-Whitney U tests for TB and context comparisons. The non-monotonic pattern observed in the descriptive analysis, with 75% MPR scenarios consistently showing higher mean TTC and lower critical conflict proportions than both adjacent MPR levels, was examined through these directional tests. The tests are confirmatory of a pattern consistent with the known L2/L3 fleet composition gradient embedded in the experimental design, in which 75% MPR corresponds to the highest Level 3 share within the automated sub-fleet (60%), but are acknowledged to be exploratory-confirmatory in nature rather than strictly a priori hypotheses. Bonferroni correction was applied to the two directional comparisons, yielding adjusted p-values of $p = 0.028$ (75% MPR > 50% MPR) and $p = 0.016$ (75% MPR > 100% MPR), both remaining below the 0.05 threshold. Effect sizes were quantified using the rank-biserial correlation r.

Both analytical streams, traffic indicators and conflict-level TTC, are derived from the same representative replication per scenario, ensuring that traffic and safety outcomes are evaluated under identical simulated conditions. The traffic analysis provides a network-wide characterisation of how MPR and TOR conditions shape traffic flow, while the conflict analysis quantifies safety implications at the interaction level. Together they allow a joint assessment of whether the factors that drive operational change also drive safety change, and whether the two dimensions converge on the same conclusions regarding the relative importance of MPR, TB, and TOR context.

3. Results

3.1. Traffic Performance

3.1.1. Overview and Sensitivity to Context and TB

Table 2 presents the five traffic indicators for all 18 scenarios with percentage changes from the Baseline LC reference. Figure 3 visualises the MPR gradient for each indicator across the four scenario combinations of context and TB. Spearman correlations between MPR and the traffic indicators (TOR scenarios only) are strong to very strong for four of the five indicators: Speed ($\rho = -0.972$, $p < 0.001$), Lane Changes ($\rho = -0.970$, $p < 0.001$), Travel Time ($\rho = 0.972$, $p < 0.001$), and Density ($\rho = 0.995$, $p < 0.001$), confirming highly systematic MPR-driven trends. Delay Time yielded $\rho = -0.777$ ($p < 0.001$), reflecting its non-monotonic response discussed below. Two observations are immediately apparent from Figure 3: Lane Closure and ODD Exit lines are visually superimposed across all five panels (maximum speed difference 0.06 km/h at any matched MPR and TB level), and Regular and Extended TB lines are likewise indistinguishable (maximum speed difference 0.30 km/h, maximum delay difference 0.11 s/km). Neither the TOR context nor the TB duration therefore exerts a materially different influence on network-level traffic performance.

All four scenario lines are nearly indistinguishable within each panel, confirming null TB and context effects. Figure 3b reveals the non-monotonic delay response peaking at 50% MPR.

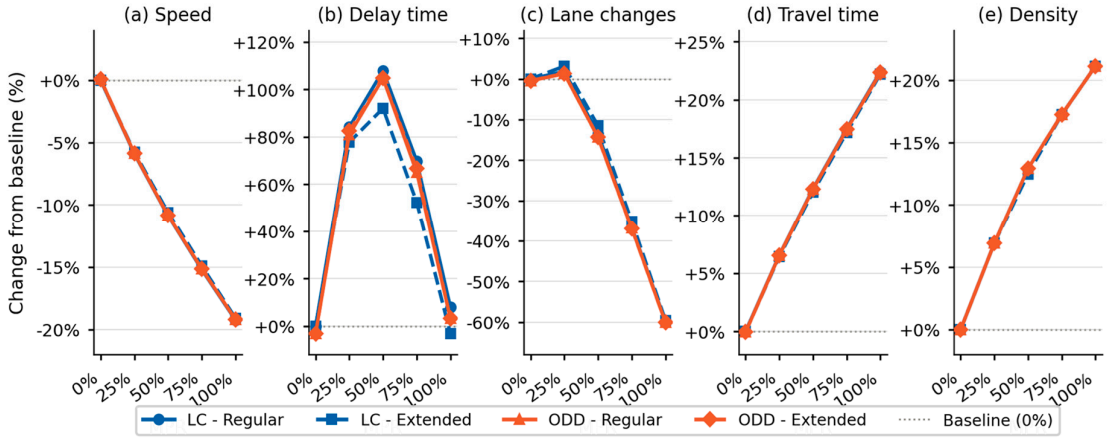


Figure 3. Percentage change from baseline (Scenario 1, Baseline LC) in five network-level traffic performance indicators across MPR levels, by TOR context (LC: Lane Closure, ODD: ODD Exit) and Time Budget condition (Regular/Extended): (**a**) speed; (**b**) delay time; (**c**) lane changes; (**d**) travel time; (**e**) density.

3.1.2. Speed, Travel Time, and Density

Network mean speed declined monotonically from 100.39 km/h at baseline to 81.08 km/h at 100% MPR (−19.2%), with consistent intermediate values across contexts and TB conditions. Travel time increased from 36.43 s/km to 44.60 s/km (+22.4%), and vehicle density rose from 2.32 to 2.81 veh/km (+21.1%).

The monotonic speed reduction with increasing MPR reflects primarily the more conservative behavioural parameters of automated vehicles, including shorter clearance, tighter gap acceptance, and smoother but slower longitudinal control, which lower aggregate network speed as AVs progressively replace human-driven passenger cars. TOR events contribute an additional localised speed reduction in the trigger zone, where post-TOR deceleration creates transient speed differentials with surrounding traffic. However, this effect is spatially concentrated and secondary to the fleet composition effect observed at the network level. It is further noted that vehicles travelling at lower speeds at the moment of TOR triggering naturally produce shorter braking distances and smaller speed differentials, a physical relationship captured implicitly through the profile-specific deceleration parameters rather than through an explicit speed-dependent TB specification.

Figure 4 places all 18 operating points on the speed-density diagram. All scenarios lie on the free-flow branch of the fundamental relationship, with LC and ODD scenarios nearly superimposed at each MPR level. The operating points follow a tight linear trend, confirming that the corridor never approached capacity under any simulated condition and that the speed reduction reflects behavioural conservatism during TOR transitions rather than congestion onset.

3.1.3. Delay Time

Delay time exhibited the most analytically distinctive pattern. Starting from 0.63 s/km at baseline, it rose to 1.16 s/km (+84.1%) at 25% MPR and peaked at 1.31 s/km (+107.9%) at 50% MPR, before declining to 1.07 s/km (+69.8%) at 75% MPR and converging near baseline at 0.68 s/km (+7.9%) at 100% MPR. This inverted-U pattern, visible in panel (b) of Figure 3, was consistent across all four scenario combinations and is attributed to maximum fleet heterogeneity at intermediate penetration rates: behavioural differences between automated and human-driven vehicles generate the greatest speed differentials and flow disruption when neither type dominates the fleet. The negative Spearman correlation ($\rho = -0.777$) reflects the net downward trend when the 100% MPR return-to-baseline is included, masking the non-monotonicity in the mid-range.

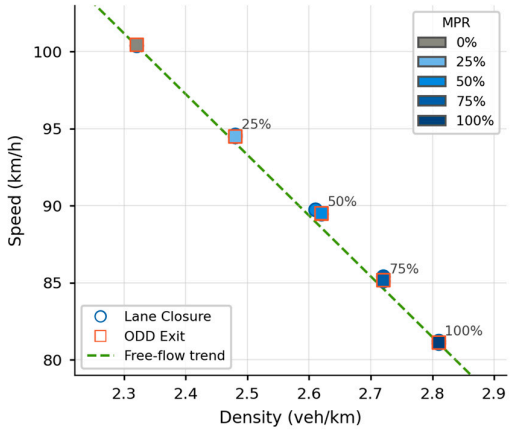


Figure 4. Speed-density operating points for all 18 simulation scenarios. Fill colour indicates MPR level (grey: baseline 0%, light to dark blue: 25% to 100%). Circle markers denote Lane Closure scenarios, squares denote ODD Exit scenarios. The dashed green line shows the free-flow trend. LC and ODD markers are nearly superimposed at each MPR level.

3.1.4. Lane-Changing Activity

Lane-changing frequency remained near-baseline at 25% MPR (+1.8%), then declined steeply: −13.5% at 50% MPR, −36.7% at 75% MPR, and −59.8% at 100% MPR. The threshold effect at 25% MPR, where a small AV share does not alter aggregate lane-change patterns, and the near-linear decline thereafter are clearly visible in panel (c) of Figure 3. At 100% MPR, car-type lane changes drop to zero as all passenger cars are replaced by automated vehicles. However, the residual network activity of 41.98 #/km reflects a combination of AV lane changes at merge zones and TOR trigger sections (63% of residual) and lane changes by trucks, buses, and motorcycles, which retained human-driving parameters throughout (37% of residual).

3.2. Safety Conflict Analysis

The following section examines whether the MPR effects and TB and context effects identified operationally are echoed in the safety conflict data.

3.2.1. Conflict Characteristics

A total of 674 conflict events were identified across all 18 scenarios. Of these, 663 (98.4%) were rear-end conflicts, 10 (1.5%) lane-change conflicts, and 1 (0.1%) crossing conflict. TTC is discretised at 0.1 s intervals, with 23.1% of events at the SSAM lower bound of 0.2 s. Mean TTC across all scenarios was 0.696 s (SD = 0.444 s), the proportion of critical conflicts (TTC $\leq$ 0.5 s) was 46.2% across TOR scenarios versus 43.9% at baseline. Table 3 presents the full conflict summary by scenario.

Vehicle-km decreases slightly with increasing MPR (range: 36,462 to 38,725 km), reflecting the more conservative longitudinal behaviour of automated vehicles, conflict rates account for this variation rather than assuming constant exposure.

Exposure-normalised conflict rates, expressed as conflicts per 1000 vehicle-km, are reported in Table 3 alongside TTC severity indicators. Vehicle-km was estimated from the Total Distance Travelled output of Aimsun Next for each scenario (range: 36,462 to 38,725 km), accounting for the slight reduction in vehicle-km at higher MPR levels due to the more conservative behaviour of automated vehicles. Conflict frequency and severity do not always co-vary: Scenario 8 (Lane Closure, 75% MPR, Extended TB) produces both the lowest conflict rate (0.67 per 1000 vehicle-km) and the highest mean TTC (0.784 s), indicating both fewer and less severe interactions. While Scenario 5 (Lane Closure, 100% MPR, Regular TB) produces the highest conflict rate (1.29 per 1000 vehicle-km) alongside a lower mean

TTC (0.609 s) and the highest proportion of critical conflicts (53.2%), indicating both more frequent and more severe interactions. Baseline scenarios produce rates of 0.72 to 0.75 per 1000 vehicle-km, below the mean TOR scenario rate of 1.03 per 1000 vehicle-km, indicating that TOR conditions are associated with higher conflict frequency on average. The severity picture is more nuanced: scenarios at 25% and 75% MPR show higher mean TTC than baseline (0.741 s and 0.765 s respectively, compared with 0.702 s at baseline), indicating that while TOR events increase conflict frequency, severity at lower and intermediate automation shares does not necessarily exceed baseline human-driven conditions. Scenarios at 50% and 100% MPR are consistently worse than baseline on both dimensions, both more frequent and more severe. Pooled by MPR level across TOR scenarios, conflict rates are 1.063 at 25% MPR, 1.114 at 50% MPR, 0.835 at 75% MPR, and 1.097 at 100% MPR, mirroring the non-monotonic pattern observed in the TTC severity analysis and reinforcing the interpretation of 75% MPR as a local safety optimum under the simulated conditions.

Table 3. Conflict-level TTC descriptive statistics by scenario.

Sc.	Context	MPR	TB	N	Rate (Conf./1000 veh-km)	Mean TTC (s)	SD	Median (s)	log(TTC)	TTC $\leq$ 0.5 s (%)
1	**Baseline LC**	**0%**	**–**	29	0.749	0.724	0.457	0.70	−0.564	41.4
2	LC	25%	Reg	42	1.096	0.748	0.477	0.75	−0.556	42.9
3	LC	50%	Reg	44	1.160	0.659	0.446	0.55	−0.668	50.0
4	LC	75%	Reg	37	0.992	0.714	0.435	0.70	−0.566	43.2
5	LC	100%	Reg	47	1.289	0.609	0.374	0.50	−0.697	53.2
6	LC	25%	Ext	41	1.069	0.749	0.485	0.80	−0.562	43.9
7	LC	50%	Ext	42	1.106	0.681	0.462	0.55	−0.641	50.0
8	LC	75%	Ext	25	0.669	0.784	0.436	0.80	−0.445	32.0
9	LC	100%	Ext	34	0.932	0.647	0.408	0.65	−0.659	47.1
10	**Baseline ODD**	**0%**	**–**	28	0.723	0.679	0.450	0.70	−0.643	46.4
11	ODD	25%	Reg	41	1.070	0.722	0.483	0.70	−0.608	46.3
12	ODD	50%	Reg	42	1.108	0.645	0.462	0.40	−0.713	54.8
13	ODD	75%	Reg	35	0.938	0.774	0.425	0.80	−0.445	31.4
14	ODD	100%	Reg	38	1.042	0.653	0.414	0.55	−0.646	50.0
15	ODD	25%	Ext	39	1.018	0.746	0.498	0.80	−0.579	46.2
16	ODD	50%	Ext	41	1.081	0.624	0.460	0.40	−0.742	58.5
17	ODD	75%	Ext	28	0.751	0.804	0.443	0.85	−0.422	32.1
18	ODD	100%	Ext	41	1.124	0.671	0.417	0.60	−0.614	43.9

N = number of SSAM-identified conflicts. TTC $\leq$ 0.5 s (%) = proportion of critical interactions. log(TTC) = natural logarithm of mean TTC per scenario. Baseline scenarios shown in bold. Conflict rate = N conflicts per 1000 vehicle-km. Vehicle-km derived from Total Distance Travelled (All vehicles) output from Aimsun Next for each scenario.

3.2.2. Statistical Test Results

Table 4 summarises all statistical test results. The Kruskal-Wallis test on log(TTC) across MPR levels yielded H = 7.225 (p = 0.065), indicating a marginal aggregate effect that does not reach conventional significance, consistent with the non-monotonic rather than directional nature of the MPR-TTC relationship. To directly test the non-monotonicity, one-sided Mann-Whitney U tests were applied to examine whether 75% MPR produces higher TTC than adjacent levels. Both comparisons remained significant after Bonferroni correction for the two directional tests: 75% MPR > 50% MPR (U = 12,134; p adj = 0.028; r = −0.149) and 75% MPR > 100% MPR (U = 11,658; p adj = 0.016; r = −0.166). The effect sizes associated with these comparisons are modest, reflecting relatively small absolute TTC differences between MPR levels, the finding is considered meaningful primarily because of its consistency across all four scenario combinations of TOR context and TB configuration rather than the magnitude of individual pairwise contrasts. This pattern was consistent across both contexts and both TB conditions (Table 3: mean TTC at 75% MPR ranges

from 0.71 to 0.80 s, compared with 0.62–0.68 s at 50% MPR and 0.61–0.67 s at 100% MPR). TB (U = 46,422; p = 0.645) and context (U = 47,220; p = 0.870) comparisons were both non-significant with negligible effect sizes (r $\leq$ 0.021).

Table 4. Statistical test results for MPR effects on TTC and traffic indicators.

Comparison/Test	Statistic	df/N	*p*-Value	Effect Size	Interpretation
Kruskal-Wallis: MPR effect on log(TTC) (4 levels, TOR only)	H = 7.225	df = 3	p = 0.065	–	Marginal, non-monotonic pattern
Mann-Whitney: 75% MPR > 50% MPR on log(TTC) (one-sided)	U = 12,134	–	p = 0.028	r = −0.149	Significant (Bonferroni-adjusted)
Mann-Whitney: 75% MPR > 100% MPR on log(TTC) (one-sided)	U = 11,658	–	p = 0.016	r = −0.166	Significant (Bonferroni-adjusted)
Mann-Whitney: TB Regular vs. Extended on log(TTC)	U = 46,422	N = 617	p = 0.645	r = 0.021	Not significant
Mann-Whitney: LC vs. ODD Exit on log(TTC)	U = 47,220	N = 617	p = 0.870	r = 0.008	Not significant
Spearman: MPR vs. Speed (operational, TOR scenarios)	ρ = −0.972	N = 16	p < 0.001	–	Very strong
Spearman: MPR vs. Delay Time (operational, TOR scenarios)	ρ = −0.777	N = 16	p < 0.001	–	Strong, non-monotonic in sign
Spearman: MPR vs. Lane Changes (operational, TOR scenarios)	ρ = −0.970	N = 16	p < 0.001	–	Very strong
Spearman: MPR vs. Travel Time (operational, TOR scenarios)	ρ = +0.972	N = 16	p < 0.001	–	Very strong
Spearman: MPR vs. Density (operational, TOR scenarios)	ρ = +0.995	N = 16	p < 0.001	–	Very strong

r = rank-biserial correlation (effect size for Mann-Whitney tests). Spearman ρ computed on TOR scenario means (N = 16), MPR vs. traffic indicators. One-sided tests for the 75% MPR directional hypotheses, all other tests two-sided. Bonferroni correction applied to the two directional comparisons (adjusted p-values reported), all other comparisons are single tests requiring no adjustment. The directional tests are acknowledged to be exploratory-confirmatory in nature, motivated by the non-monotonic pattern observed in the descriptive analysis and consistent with the known L2/L3 fleet composition gradient at 75% MPR.

4. Discussion

4.1. Traffic Implications

The traffic findings present a coherent picture of how AV penetration reshapes motorway performance under TOR-constrained mixed-traffic conditions. The very strong Spearman correlations between MPR and four of the five indicators ($|\rho| \geq 0.97$) confirm that these changes are systematic and MPR-driven rather than scenario-specific. The speed reduction and travel time increase reflect the more conservative headways and stricter lane discipline of automated vehicles operating under post-TOR behavioural profiles, a direct consequence of the empirically derived parameter sets used in the simulation. Crucially, the speed-density analysis confirms that none of these changes represent capacity constraint: the corridor remains in free-flow throughout the MPR range, and the operating points move linearly down the free-flow branch as penetration increases. The non-monotonic delay response, peaking at 50% MPR, is the most theoretically significant operational finding. It provides microsimulation evidence for the compositional heterogeneity hypothesis: delay is generated not by automation per se but by the behavioural mismatch between automated and human-driven vehicles, which is maximal at intermediate penetration rates. Highway operators should therefore anticipate a temporary worsening of delay during the mid-range transition period, with partial recovery only as penetration approaches 100%. The 60% reduction in lane-changing activity at full MPR has a complementary implication: traffic management strategies calibrated to human-driver gap-acceptance behaviour (such as variable message signs, ramp metering, and mandatory lane assignments) may require

recalibration as AV penetration grows. Notably, network flow remains essentially constant across all MPR levels, consistent with free-flow conditions throughout, the operational deterioration in speed and travel time therefore reflects behavioural conservatism of automated vehicles rather than a capacity constraint, which has different infrastructure implications than congestion-driven delay.

4.2. Safety Implications and the Non-Monotonic MPR Effect

The confirmation of a statistically significant TTC advantage at 75% MPR over both adjacent levels is a substantive safety finding. The directional Mann-Whitney tests ($p = 0.028$ and $p = 0.016$, rank-biserial $r \approx -0.15$ to -0.17) establish that this non-monotonicity is not a sampling artefact but a consistent structural feature of the data, replicated across both TOR contexts and both TB conditions. Level 3 vehicles, which dominate the automated sub-fleet at this MPR level, are characterised by shorter reaction times, tighter headway control, and smoother deceleration profiles than Level 2 or human-driven vehicles, offering a plausible compositional explanation for the observed pattern. The local safety maximum observed at 75% MPR is associated with a fleet composition in which Level 3 vehicles constitute 45% of the total fleet and 60% of the automated sub-fleet, alongside 30% Level 2 vehicles and 25% HDVs. Since MPR and L2/L3 composition co-vary by design, the observed TTC pattern cannot be attributed uniquely to either factor in isolation, rather, it reflects the joint effect of total automation penetration and the specific fleet composition that characterises the 75% MPR deployment scenario under the adopted market trajectory. Disentangling these effects would require a factorial design varying MPR and L2/L3 composition independently, which is recommended as a priority direction for future work.

This interpretation is consistent with the companion spatial GAM [50], which showed that automated vehicles as the first conflict vehicle produce significantly higher TTC than human-driven vehicles across all behavioural profiles, with Level 3 Nervous yielding the largest effect. The null results for TB and context are consistent across both outcome domains. This traffic-safety convergence is notable: both the TOR trigger type and the TB duration produce negligible effects at the network level, with maximum traffic differences not exceeding 0.30 km/h in speed and 0.11 s/km in delay, and statistically non-significant TTC differences with effect sizes below $r = 0.03$. From a regulatory standpoint, this suggests that modest extensions to standard TB requirements are unlikely to yield measurable network-level improvements, and that TOR management should focus on the MPR transition period, particularly around 50% MPR where delay peaks, and between 50% and 100% MPR where lane-changing activity declines most sharply.

4.3. Limitations

The analysis is based on a single 50 km motorway corridor under peak-hour demand, and results may not generalise to other network types, demand levels, or geometric configurations, replication across diverse corridors is necessary before broader conclusions can be drawn. While the findings are derived from a specific calibrated corridor, the simulated conditions, a high-speed continuous-flow motorway with mixed vehicle composition, peak-hour demand, and geometry/capability-driven TOR triggers, are representative of a broad class of European motorway environments, the operational and safety patterns identified are therefore expected to be relevant to similar corridor types, with the understanding that the precise magnitudes of the effects may vary with local geometric configuration, demand level, and driving culture.

Each scenario was simulated using ten replications, with the replication closest to the cross-replication mean travel time selected for both traffic and safety indicator extraction. Pooling conflicts across all replications was deliberately avoided, as doing so would

artificially inflate the effective sample size by treating correlated repetitions of the same simulation environment as independent observations. The selected replication may not be fully representative of the cross-replication distribution of conflict frequency or TTC severity. Future work should retain full replication sets and apply mixed-effects or hierarchical models to quantify stochastic variability in safety outcomes across replications. TTC and PET are the sole surrogate safety indicators, complementary measures such as delta-V would capture additional dimensions of conflict severity and should be incorporated in future extensions. The TTC distribution is discretised at 0.1 s intervals and left-censored at a lower bound of 0.2 s, which collapses the most severe interactions into a single bin and may reduce test power for detecting differences in the critical lower tail. The safety analysis was limited to TTC as the primary analysed surrogate indicator. While PET was used as a conflict screening threshold, it was not analysed as an outcome variable given the predominantly rear-end conflict geometry of the corridor, for which TTC provides greater discriminatory power. Complementary indicators such as delta-V, which captures the kinetic severity of potential collisions, would enrich the assessment and are recommended for future extensions.

Only planned, system-initiated TOR events with a defined time budget were modelled, emergency disengagements requiring a Minimum Risk Manoeuvre constitute a distinct operational condition and were outside the scope of this framework. Behavioural parameters for automated and post-TOR manual driving were sourced from prior microsimulation and driving simulator studies, as real-world naturalistic trajectory data for L2/L3 vehicles in mixed-traffic highway conditions at the granularity required for microsimulation parameterisation is not yet publicly available. Validation against real-world AV fleet data remains an important direction for future work as deployment expands and such data become accessible. The Time Budget was held constant across MPR levels in this study. Future work should examine speed-adaptive TB specifications in which the available response time is adjusted as a function of instantaneous vehicle speed at the point of TOR triggering, which would more precisely reflect the relationship between entry speed, stopping distance, and driver readiness during automation disengagement.

The non-parametric tests applied to TTC treat individual conflict events as the unit of analysis, while each conflict represents a distinct vehicle-pair interaction, conflicts within the same scenario share experimental conditions, introducing within-scenario correlation that may slightly underestimate standard errors. A mixed-effects model with scenario as a random effect would address this dependency more formally and is recommended for future extensions of this framework.

5. Conclusions

This study quantified the network-level traffic and safety effects of AV market penetration under take-over conditions on a calibrated 50 km Greek motorway, using 18 microsimulation scenarios, five network-level performance indicators, and 674 SSAM-derived conflict events. The findings are synthesised below across three analytical dimensions: the dominant role of MPR, the null effects of TOR context and Time Budget, and the practical implications for mixed-traffic management.

MPR is the dominant driver of all traffic outcomes, with very strong Spearman correlations ($|\rho| \geq 0.97$) for speed, lane changes, travel time, and density. Increasing AV penetration from 0% to 100% reduces network mean speed by 19.2% (from 100.39 to 81.08 km/h), increases density by 21.1% (from 2.32 to 2.81 veh/km), and raises travel time per kilometre by 22.4% (from 36.43 to 44.60 s/km). These changes are systematic and consistent across both TOR contexts and both TB conditions, with context differences not exceeding 0.06 km/h in speed and TB differences not exceeding 0.30 km/h at any MPR

level. Speed-density analysis confirms that all operating points lie on the free-flow branch of the fundamental diagram throughout the MPR range, indicating that the operational deterioration reflects the behavioural conservatism of automated vehicles under TOR transitions rather than any approach toward capacity constraint. Lane-changing frequency declined by 59.8% at full MPR, with the effect concentrated beyond 25% MPR, implying a threshold below which a small AV share does not materially alter aggregate lane-change patterns. Delay time exhibited the most theoretically distinctive response: a non-monotonic inverted-U pattern peaking at 50% MPR (+107.9% relative to baseline) and converging near baseline at 100% MPR. This behaviour is attributed to maximum fleet heterogeneity at intermediate penetration rates, where behavioural mismatch between automated and human-driven vehicles is greatest. Highway operators should therefore anticipate temporary delay worsening during the transition from low to moderate AV penetration, with meaningful recovery only as the fleet becomes predominantly automated. Traffic management strategies calibrated to human-driver gap-acceptance and lane-choice behaviour may require recalibration as AV penetration grows beyond the 50–75% threshold.

Safety analysis reveals a marginal overall MPR effect on log-transformed TTC (Kruskal-Wallis H = 7.225, $p = 0.065$), driven by a non-monotonic pattern rather than a simple directional trend. Directional Mann-Whitney tests confirm that 75% MPR scenarios produce significantly higher mean TTC than both 50% MPR (U = 12,134; $p = 0.028$; r = -0.149) and 100% MPR (U = 11,658; $p = 0.016$; r = -0.166), indicating a local safety maximum at 75% MPR that is consistent across all four scenario combinations. This pattern is consistent with the higher Level 3 share at that penetration level (45% of the total fleet), where more predictable automated trajectories may reduce interaction severity even in the presence of take-over events. Network-level corridor averages weaken the spatially localised TOR effects identified in the companion GAM study, mean TTC differences between baseline and TOR scenarios are negligible at the corridor scale, suggesting that spatially targeted interventions near TOR trigger zones and merge areas are more appropriate than corridor-wide policy responses.

Neither the TOR context (Lane Closure vs. ODD Exit) nor the TB duration (Regular vs. Extended) produces statistically significant effects on traffic indicators or TTC distributions, with negligible effect sizes across all comparisons ($r \leq 0.021$). These null results across two outcome domains and two experimental factors suggest that, at the network level, the type of TOR event and the available driver response time matter considerably less than the MPR composition of the fleet. Under the simulated conditions, TB duration does not produce detectable differences in network-level traffic or safety outcomes, suggesting that the network-level consequences of take-over events are driven more by fleet composition than by the specific response time available to the driver. Future research should extend this framework to additional corridor types and demand conditions, incorporate complementary surrogate safety indicators such as PET and delta-V, and validate the simulated dynamics using naturalistic or connected-vehicle trajectory data as AV deployments expand.

Author Contributions: Conceptualization, M.S.; methodology, M.S. and D.N.; software, M.S.; validation, M.S., D.N. and G.Y.; formal analysis, M.S.; investigation, M.S.; resources, G.Y.; data curation, M.S.; writing—original draft preparation, M.S. and D.N.; writing—review and editing, M.S. and D.N.; visualization, M.S.; supervision, G.Y. All authors have read and agreed to the published version of the manuscript.

Funding: This research received no external funding.

Institutional Review Board Statement: Not applicable.

Informed Consent Statement: Not applicable.

Data Availability Statement: The data presented in this study are available on request from the corresponding author. The data are not publicly available due to a data-sharing agreement with Nea Odos S.A., which restricts redistribution of the underlying network and traffic data.

Acknowledgments: The authors gratefully recognise Nea Odos S.A. for providing access to real highway data and network information that supported the calibration of the simulation environment.

Conflicts of Interest: The authors declare no conflicts of interest.

References

1. Yao, Z.; Hu, R.; Jiang, Y.; Xu, T. Stability and Safety Evaluation of Mixed Traffic Flow with Connected Automated Vehicles on Expressways. *J. Saf. Res.* **2020**, *75*, 262–274. [CrossRef]
2. Talebpour, A.; Mahmassani, H.S. Influence of Connected and Autonomous Vehicles on Traffic Flow Stability and Throughput. *Transp. Res. Part C Emerg. Technol.* **2016**, *71*, 143–163. [CrossRef]
3. Ye, L.; Yamamoto, T. Evaluating the Impact of Connected and Autonomous Vehicles on Traffic Safety. *Phys. A Stat. Mech. Its Appl.* **2019**, *526*, 121009. [CrossRef]
4. Mousavi, S.M.; Osman, O.A.; Lord, D.; Dixon, K.K.; Dadashova, B. Investigating the Safety and Operational Benefits of Mixed Traffic Environments with Different Automated Vehicle Market Penetration Rates in the Proximity of a Driveway on an Urban Arterial. *Accid. Anal. Prev.* **2021**, *152*, 105982. [CrossRef]
5. Arvin, R.; Khattak, A.J.; Kamrani, M.; Rio-Torres, J. Safety Evaluation of Connected and Automated Vehicles in Mixed Traffic with Conventional Vehicles at Intersections. *J. Intell. Transp. Syst.* **2021**, *25*, 170–187. [CrossRef]
6. Sauciur, N.; Molan, A.M.; Sajjadi, S.; Liu, B.; Pande, A. Evaluating Urban Network Efficiency and Safety Impacts of Connected and Autonomous Vehicles in Complex City Environments. *Transp. Res. Interdiscip. Perspect.* **2025**, *32*, 101538. [CrossRef]
7. Shin, S.; Cho, Y.; Lee, S.; Park, J. Assessing Traffic-Flow Safety at Various Levels of Autonomous-Vehicle Market Penetration. *Appl. Sci.* **2024**, *14*, 5453. [CrossRef]
8. Sinha, A.; Chand, S.; Wijayaratna, K.P.; Virdi, N.; Dixit, V. Comprehensive Safety Assessment in Mixed Fleets with Connected and Automated Vehicles: A Crash Severity and Rate Evaluation of Conventional Vehicles. *Accid. Anal. Prev.* **2020**, *142*, 105567. [CrossRef]
9. Taheri, A.; Yang, J.; Müller, S.; Milakis, D.; Quddus, M. Advancing Safety through Connected and Autonomous Vehicles: A Meta-Analysis of Market Penetration and Safety Improvement Rates from 2015 to 2024. *Eur. Transp. Res. Rev.* **2026**, *18*, 9. [CrossRef]
10. Yang, X.; Zou, Y.; Chen, L. Operation Analysis of Freeway Mixed Traffic Flow Based on Catch-up Coordination Platoon. *Accid. Anal. Prev.* **2022**, *175*, 106780. [CrossRef]
11. Papadoulis, A.; Quddus, M.; Imprialou, M. Evaluating the Safety Impact of Connected and Autonomous Vehicles on Motorways. *Accid. Anal. Prev.* **2019**, *124*, 12–22. [CrossRef]
12. Antonakaki, A.; Oikonomou, M.G.; Garefalakis, T.; Yannis, G. Driving Automation Systems Penetration and Traffic Safety: Implications for Infrastructure Design and Policy. *Infrastructures* **2024**, *9*, 234. [CrossRef]
13. Wang, T.; Guo, Q.; He, C.; Li, H.; Xu, Y.; Wang, Y.; Jiao, J. Impact of Connected and Automated Vehicles on Longitudinal and Lateral Performance of Heterogeneous Traffic Flow in Shared Autonomy on Two-Lane Highways. In Proceedings of the WCX SAE World Congress Experience, Detroit, MI, USA, 1 April 2025; p. 8098.
14. Qin, Y.; Luo, Q.; Wang, H. Stability Analysis and Connected Vehicles Management for Mixed Traffic Flow with Platoons of Connected Automated Vehicles. *Transp. Res. Part C Emerg. Technol.* **2023**, *157*, 104370. [CrossRef]
15. Mahmassani, H.S. 50th Anniversary Invited Article—Autonomous Vehicles and Connected Vehicle Systems: Flow and Operations Considerations. *Transp. Sci.* **2016**, *50*, 1140–1162. [CrossRef]
16. Zhang, M.; Uno, N.; Yang, X. Traffic Safety Evaluation for Mixed Traffic Flow Caused by Degradation of Connected Automated Vehicles. *Phys. A Stat. Mech. Its Appl.* **2025**, *659*, 130353. [CrossRef]
17. Yao, Z.; Deng, H.; Chen, Z.; He, X.; Ai, Y.; Wu, Y. Linear Internal Stability for Mixed Traffic Flow of CAVs with Different Automation Levels. *Phys. A Stat. Mech. Its Appl.* **2024**, *642*, 129759. [CrossRef]
18. Gan, J.; Ma, H.; Li, L.; Qu, X.; Ran, B. Linear Stability of Heterogeneous Traffic Flow Incorporating V2X Communication and Intraplatoon Spatial Distribution. *IEEE Internet Things J.* **2024**, *11*, 41033–41048. [CrossRef]
19. Rosca, M.A.; Oprea, F.C.; Dragu, V.; Dinu, O.M.; Costea, I.; Burciu, S. Evaluating the Impact of Automated Vehicle Penetration on Intersection Traffic Flow: A Microsimulation-Based Approach. *Systems* **2025**, *13*, 751. [CrossRef]
20. Fang, X.; Li, H.; Tettamanti, T.; Eichberger, A.; Fellendorf, M. Effects of Automated Vehicle Models at the Mixed Traffic Situation on a Motorway Scenario. *Energies* **2022**, *15*, 2008. [CrossRef]
21. Kim, J.; Lim, D.; Seo, Y.; So, J.; Kim, H. Influence of Dedicated Lanes for Connected and Automated Vehicles on Highway Traffic Flow. *IET Intell. Transp. Syst.* **2023**, *17*, 678–690. [CrossRef]

22. Xiao, G.; Lee, J.; Jiang, Q.; Huang, H.; Abdel-Aty, M.; Wang, L. Safety Improvements by Intelligent Connected Vehicle Technologies: A Meta-Analysis Considering Market Penetration Rates. *Accid. Anal. Prev.* **2021**, *159*, 106234. [CrossRef]
23. He, Y.; Xiang, D.; Wang, D. Traffic Safety Evaluation of Emerging Mixed Traffic Flow at Freeway Merging Area Considering Driving Behavior. *Sci. Rep.* **2025**, *15*, 10686. [CrossRef]
24. Garg, M.; Bouroche, M. Can Connected Autonomous Vehicles Improve Mixed Traffic Safety Without Compromising Efficiency in Realistic Scenarios? *IEEE Trans. Intell. Transp. Syst.* **2023**, *24*, 6674–6689. [CrossRef]
25. Wu, S.; Zou, Y.; Liu, D.; Chen, X.; Wang, Y.; Moeinaddini, A. Investigating Traffic Characteristics at Freeway Merging Areas in Heterogeneous Mixed-Flow Environments. *Sustainability* **2025**, *17*, 2282. [CrossRef]
26. Wang, Y.; Wang, L.; Guo, J.; Papamichail, I.; Papageorgiou, M.; Wang, F.-Y.; Bertini, R.; Hua, W.; Yang, Q. Ego-Efficient Lane Changes of Connected and Automated Vehicles with Impacts on Traffic Flow. *Transp. Res. Part C Emerg. Technol.* **2022**, *138*, 103478. [CrossRef]
27. Jiang, Y.; Ren, T.; Ma, Y.; Wu, Y.; Yao, Z. Traffic Safety Evaluation of Mixed Traffic Flow Considering the Maximum Platoon Size of Connected Automated Vehicles. *Phys. A Stat. Mech. Its Appl.* **2023**, *612*, 128452. [CrossRef]
28. De Zwart, R.; Kamphuis, K.; Cleij, D. Driver Behavioural Adaptations to Simulated Automated Vehicles, Potential Implications for Traffic Microsimulation. *Transp. Res. Part F Traffic Psychol. Behav.* **2023**, *92*, 255–265. [CrossRef]
29. Yao, H.; An, S.; Zhou, H.; Itoh, M. Driver Takeover Performance in Conditionally Automated Driving: Sudden System Failure Situation versus ODD Exit Situation. *SICE J. Control Meas. Syst. Integr.* **2021**, *14*, 89–96. [CrossRef]
30. Tan, X.; Zhang, Y. The Effects of Takeover Request Lead Time on Drivers' Situation Awareness for Manually Exiting from Freeways: A Web-Based Study on Level 3 Automated Vehicles. *Accid. Anal. Prev.* **2022**, *168*, 106593. [CrossRef]
31. Weaver, B.W.; DeLucia, P.R. A Systematic Review and Meta-Analysis of Takeover Performance During Conditionally Automated Driving. *Hum. Factors* **2022**, *64*, 1227–1260. [CrossRef]
32. Wu, H.; Wu, C.; Lyu, N.; Li, J. Does a Faster Takeover Necessarily Mean It Is Better? A Study on the Influence of Urgency and Takeover-Request Lead Time on Takeover Performance and Safety. *Accid. Anal. Prev.* **2022**, *171*, 106647. [CrossRef]
33. Tanshi, F.; Söffker, D. A Quantitative Model of Takeover Request Time Budget for Conditionally Automated Driving. *IEEE Access* **2025**, *13*, 201832–201846. [CrossRef]
34. Zhang, B.; De Winter, J.; Varotto, S.; Happee, R.; Martens, M. Determinants of Take-over Time from Automated Driving: A Meta-Analysis of 129 Studies. *Transp. Res. Part F Traffic Psychol. Behav.* **2019**, *64*, 285–307. [CrossRef]
35. Pipkorn, L.; Tivesten, E.; Dozza, M. It's about Time! Earlier Take-over Requests in Automated Driving Enable Safer Responses to Conflicts. *Transp. Res. Part F Traffic Psychol. Behav.* **2022**, *86*, 196–209. [CrossRef]
36. Deng, H.; Xiang, G.; Pan, J.; Wu, X.; Fan, C.; Wang, K.; Peng, Y. How to Design Driver Takeover Request in Real-World Scenarios: A Systematic Review. *Transp. Res. Part F Traffic Psychol. Behav.* **2024**, *104*, 411–432. [CrossRef]
37. Tanshi, F.; Soffker, D. Determination of Takeover Time Budget Based on Analysis of Driver Behavior. *IEEE Open J. Intell. Transp. Syst.* **2022**, *3*, 813–824. [CrossRef]
38. Gold, C.; Happee, R.; Bengler, K. Modeling Take-over Performance in Level 3 Conditionally Automated Vehicles. *Accid. Anal. Prev.* **2018**, *116*, 3–13. [CrossRef]
39. Yang, W.; Wu, Z.; Tang, J.; Liang, Y. Assessing the Effects of Modalities of Takeover Request, Lead Time of Takeover Request, and Traffic Conditions on Takeover Performance in Conditionally Automated Driving. *Sustainability* **2023**, *15*, 7270. [CrossRef]
40. Jin, L.; Liu, X.; Guo, B.; Han, Z.; Wang, Y.; Cao, Y.; Yang, X.; Shi, J. Impact of Non-Driving Related Task Types, Request Modalities, and Automation on Driver Takeover: A Meta-Analysis. *Saf. Sci.* **2025**, *181*, 106704. [CrossRef]
41. Du, N.; Zhou, F.; Pulver, E.M.; Tilbury, D.M.; Robert, L.P.; Pradhan, A.K.; Yang, X.J. Predicting Driver Takeover Performance in Conditionally Automated Driving. *Accid. Anal. Prev.* **2020**, *148*, 105748. [CrossRef]
42. Lin, Q.; Li, S.; Ma, X.; Lu, G. Understanding Take-over Performance of High Crash Risk Drivers during Conditionally Automated Driving. *Accid. Anal. Prev.* **2020**, *143*, 105543. [CrossRef]
43. Zeeb, K.; Buchner, A.; Schrauf, M. Is Take-over Time All That Matters? The Impact of Visual-Cognitive Load on Driver Take-over Quality after Conditionally Automated Driving. *Accid. Anal. Prev.* **2016**, *92*, 230–239. [CrossRef] [PubMed]
44. Yoon, S.H.; Kim, Y.W.; Ji, Y.G. The Effects of Takeover Request Modalities on Highly Automated Car Control Transitions. *Accid. Anal. Prev.* **2019**, *123*, 150–158. [CrossRef]
45. Sekadakis, M.; Trösterer, S.; Moertl, P.; Yannis, G. Identifying Driving Profiles after Take over Request in Automated Vehicles at SAE Levels 2 and 3. *Transp. Res. Part F Traffic Psychol. Behav.* **2025**, *111*, 250–263. [CrossRef]
46. Sekadakis, M.; Yannis, G. Systematic Review and Meta-Analysis of Take-over Time from Automated Driving at SAE Levels 2 and 3 to Manual Control. *Transp. Res. Part F Traffic Psychol. Behav.* **2025**, *113*, 263–306. [CrossRef]
47. Zhang, N.; Fard, M.; Xu, J.; Davy, J.L.; Robinson, S.R. Influence of Non-Driving Related Tasks on Driving Performance after Takeover Transition in Conditionally Automated Driving. *Transp. Res. Part F Traffic Psychol. Behav.* **2023**, *96*, 248–264. [CrossRef]

48. Samani, A.R.; Mishra, S.; Dey, K. Assessing the Effect of Long-Automated Driving Operation, Repeated Take-over Requests, and Driver's Characteristics on Commercial Motor Vehicle Drivers' Driving Behavior and Reaction Time in Highly Automated Vehicles. *Transp. Res. Part F Traffic Psychol. Behav.* **2022**, *84*, 239–261. [CrossRef]
49. Lu, X.; Tan, H.; Zhang, H.; Wang, W.; Xie, S.; Yue, T.; Chen, F. Triboelectric Sensor Gloves for Real-Time Behavior Identification and Takeover Time Adjustment in Conditionally Automated Vehicles. *Nat. Commun.* **2025**, *16*, 1080. [CrossRef]
50. Sekadakis, M.; Oikonomou, M.G.; Yannis, G. Safety Effects of Take-over Requests on Vehicle Conflicts in Realistic Mixed Traffic Simulation. *Accid. Anal. Prev.* **2026**, *232*, 108520. [CrossRef]
51. Xie, H.; Tanin, E.; Karunasekera, S.; Qi, J.; Zhang, R.; Kulik, L.; Ramamohanarao, K. Quantifying the Impact of Autonomous Vehicles Using Microscopic Simulations. In Proceedings of the 12th ACM SIGSPATIAL International Workshop on Computational Transportation Science (IWCTS 2019), Chicago, IL, USA, 5 November 2019; pp. 1–10. [CrossRef]
52. Zhang, J.; Li, Y.; Guo, Y.; Ma, K. Study on Traffic Flow Characteristics in Mixed Automated and Manual Driving Conditions. In Proceedings of the 2022 China Automation Congress (CAC), Xiamen, China, 25–27 November 2022; pp. 1003–1007. [CrossRef]
53. Gettman, D.; Head, L. Surrogate Safety Measures from Traffic Simulation Models. *Transp. Res. Rec.* **2003**, *1840*, 104–115. [CrossRef]

Disclaimer/Publisher's Note: The statements, opinions and data contained in all publications are solely those of the individual author(s) and contributor(s) and not of MDPI and/or the editor(s). MDPI and/or the editor(s) disclaim responsibility for any injury to people or property resulting from any ideas, methods, instructions or products referred to in the content.